

SUPPORTING INFORMATION

Three-in-One: Achieving Robust and Effective Hydrogen-Evolving Hybrid Materials by Integrating Polyoxometalate, Photo-responsive Metal-Organic Framework, and in-situ Generated Pt nanoparticles

Le Jiao, Yuanyuan Dong, Xing Xin, Ruijie Wang, Hongjin Lv*

MOE Key Laboratory of Cluster Science, School of Chemistry and Chemical Engineering, Beijing Institute of Technology, Beijing 102488, P. R. China.

Corresponding email: hly@bit.edu.cn

Table of content

1. Figure S1-S16

Figure S1. SEM image of NU-1000.	S3
Figure S2. PXRD patterns of P_2W_{18} , 0.34- P_2W_{18} @NU-1000 and NU-1000.	S3
Figure S3. EDS elemental analysis of NU-1000.	S4
Figure S4. Photocatalytic hydrogen evolution at different pH values.	S4
Figure S5. TEM image of NU-1000-Pt.	S5
Figure S6. XPS of Pt in NU-1000-Pt.	S5
Figure S7. EDS elemental analysis of 0.34- P_2W_{18} @NU-1000-Pt.	S6
Figure S8. The corresponding elemental mapping images of 0.34- P_2W_{18} @NU-1000-Pt.	S6
Figure S9. The comparison of low temperature N_2 adsorption-desorption isotherms of 0.34- P_2W_{18} @NU-1000 before and after photocatalysis.	S7
Figure S10. The comparison of the pore distribution curves of 0.34- P_2W_{18} @NU-1000 before and after photocatalysis.	S7
Figure S11. Photocatalytic hydrogen evolution of 0.34- P_2W_{18} @NU-1000 with different types of Pt sources.	S8

Figure S12. SEM image of 0.34- P₂W₁₈ @NU-1000 after photocatalytic hydrogen evolution.	S8	
Figure S13. PXRD patterns of 0.34- P₂W₁₈ @NU-1000 before and after photocatalytic reaction.	S9	
Figure S14. FT-IR spectra of 0.34- P₂W₁₈ @NU-1000 before and after photocatalysis.	S9	
Figure S15. Photocatalytic hydrogen under different light sources.	S10	
Figure S16. Photocatalytic hydrogen evolution of 0.34- P₂W₁₈ @NU-1000 under Natural Sunlight.	S10	
Figure S17. Cyclic voltammogram of P₂W₁₈ (10^{-4} M) in 0.1 M H ₂ SO ₄ aqueous solution.	S11	
2. Table S1-S2		
Table S1. Comparison of different photocatalytic systems for hydrogen production.	S11	
Table S2. PL decay (at 505 nm) lifetimes of NU-1000, 0.34- P₂W₁₈ @NU-1000 samples upon excitation at 365 nm.	S11	
3. Apparent quantum yield calculation		S12
4. References		S12

1. Figure S1-S17

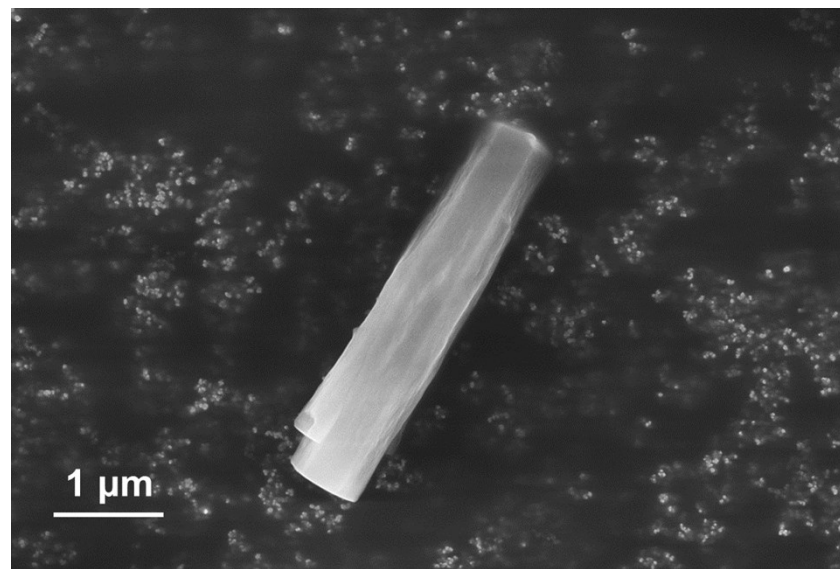


Figure S1. SEM image of NU-1000.

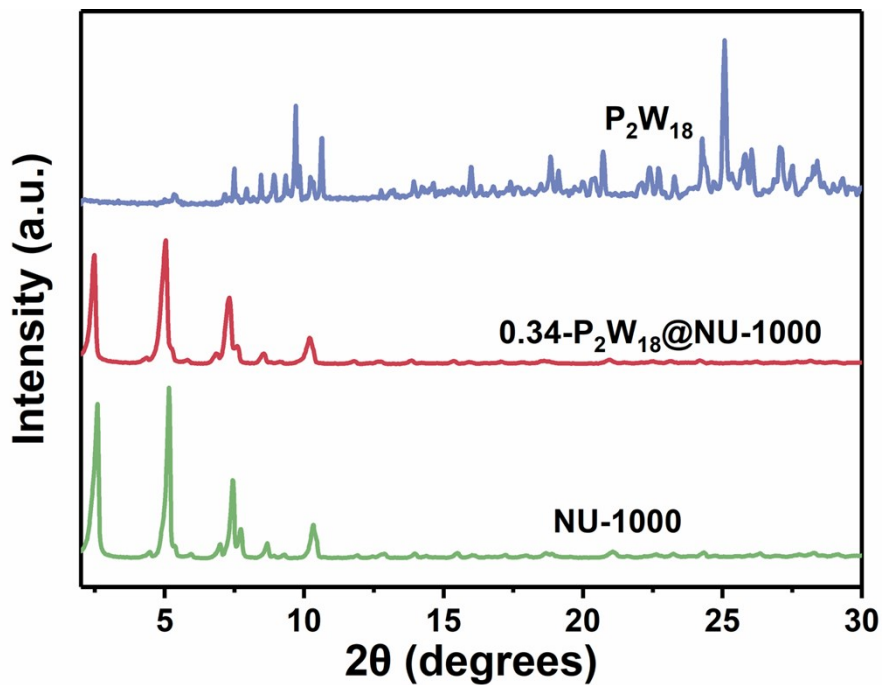


Figure S2. PXRD patterns of P₂W₁₈, 0.34-P₂W₁₈@NU-1000 and NU-1000.

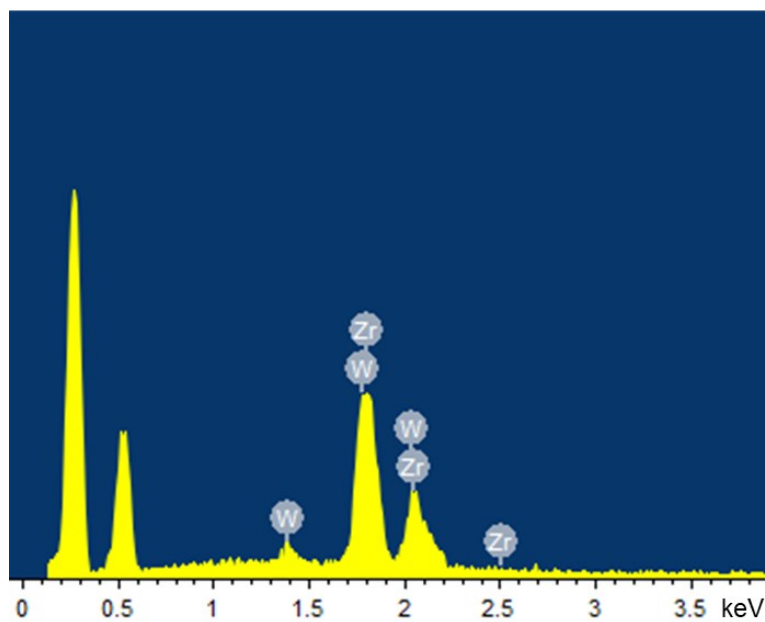


Figure S3. EDS elemental analysis of 0.34-P₂W₁₈@NU-1000.

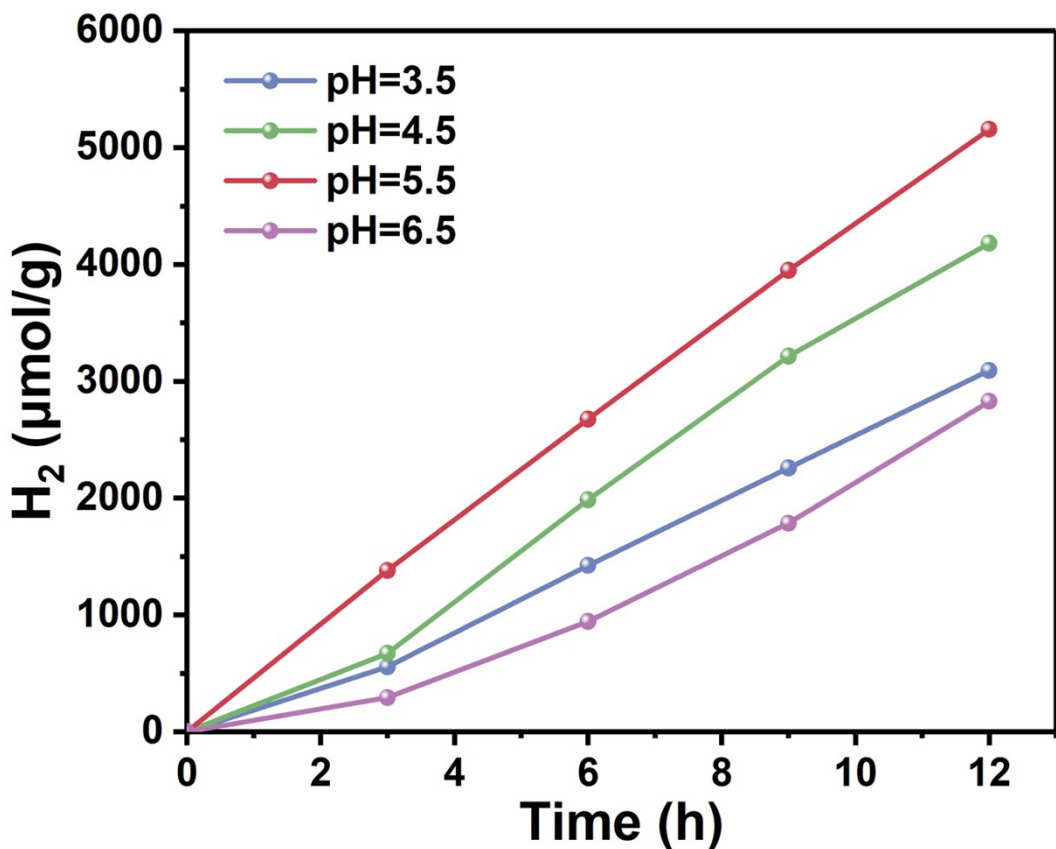


Figure S4. Photocatalytic hydrogen evolution at different pH values. Conditions: 10 mg of 0.34-P₂W₁₈@NU-1000, 1 wt% Pt, 20 mL of 1 M AA aqueous, 300 W Xe-lamp.

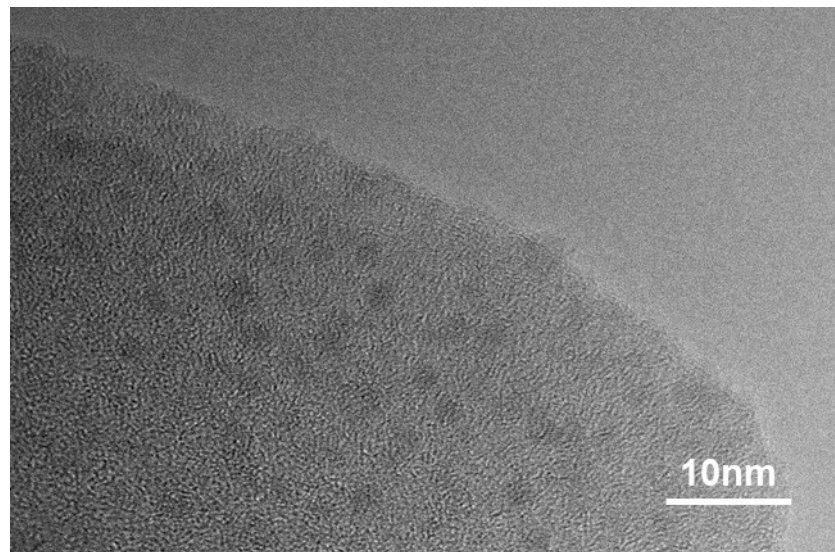


Figure S5. High resolution TEM image of NU-1000-Pt.

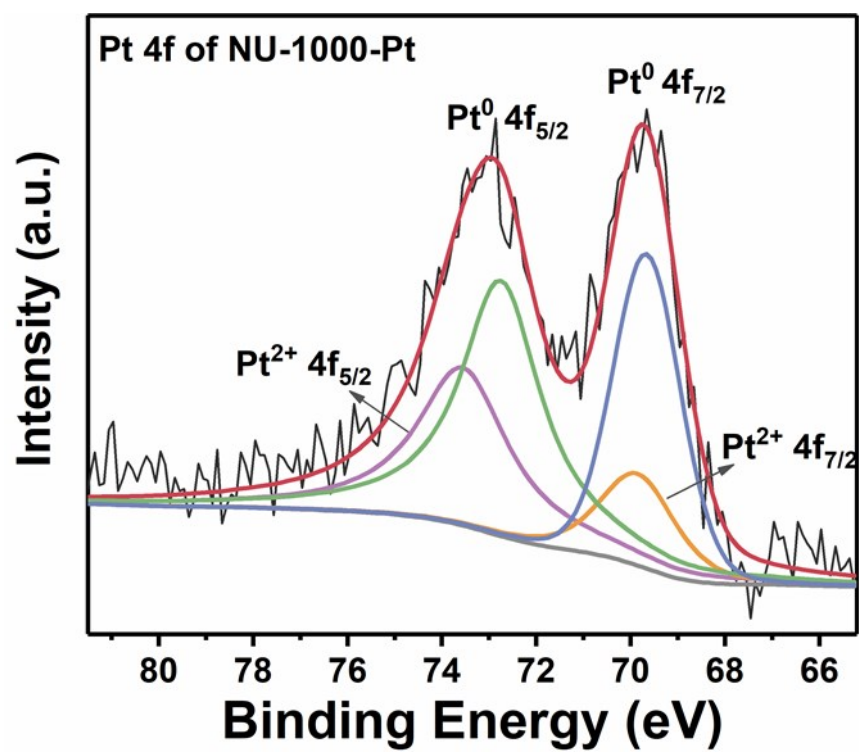


Figure S6. High resolution XPS spectra of Pt 4f in NU-1000-Pt.

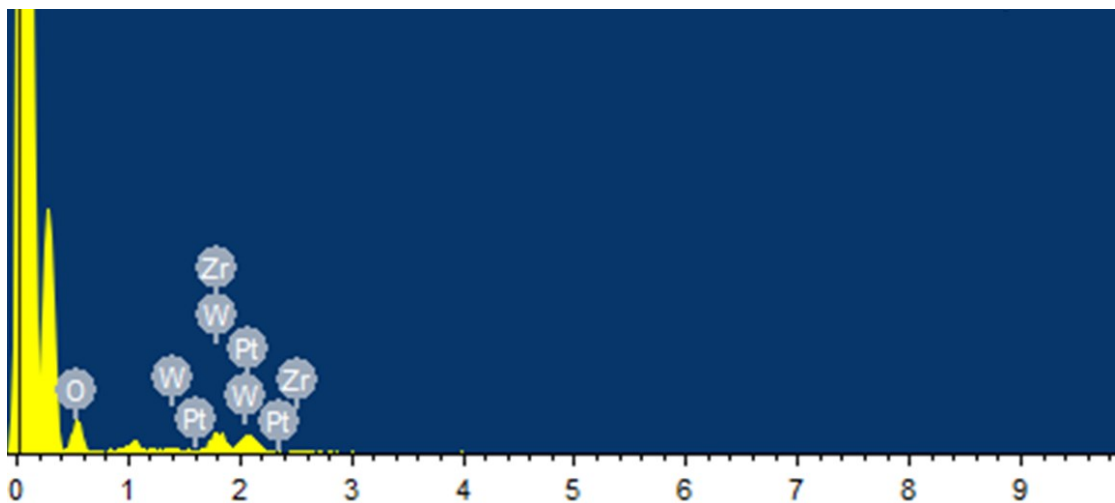


Figure S7. EDS elemental analysis of 0.34- Pt_2W_{18} @NU-1000-Pt.

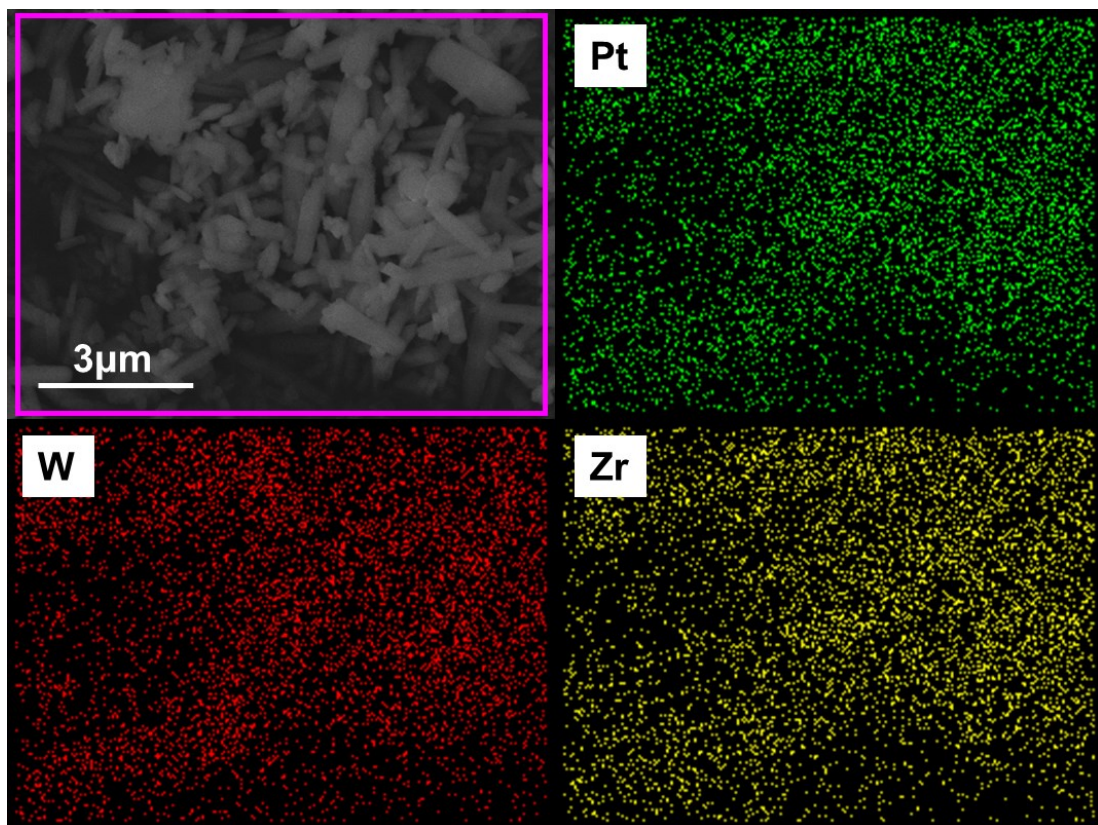


Figure S8. The corresponding elemental mapping images of 0.34- Pt_2W_{18} @NU-1000-Pt.

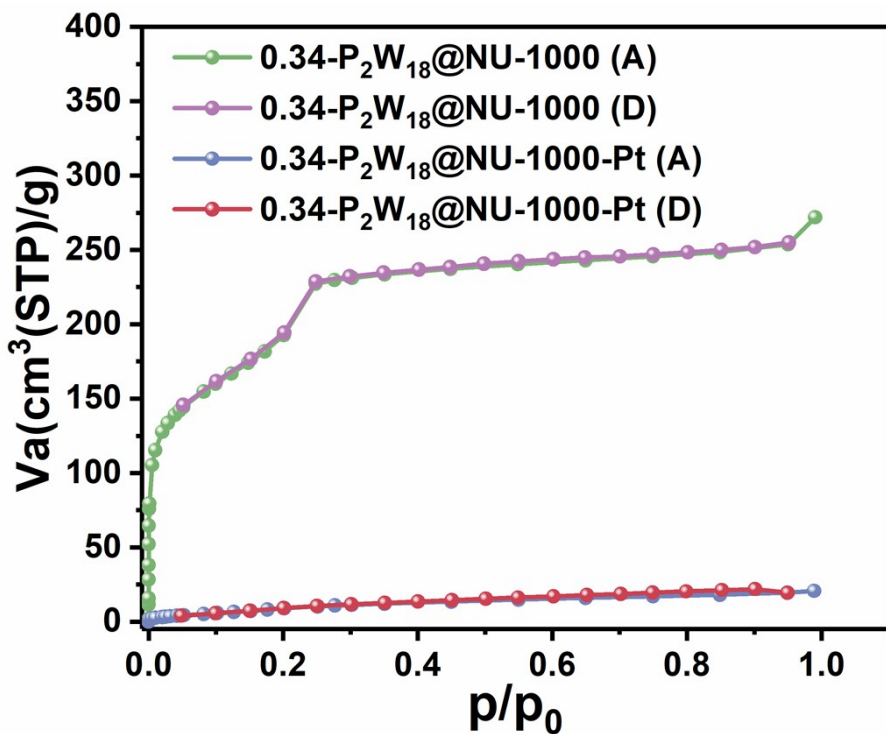


Figure S9. The comparison of low temperature N_2 adsorption-desorption isotherms of $0.34\text{-P}_2\text{W}_{18}\text{@NU-1000}$ before and after photocatalysis.

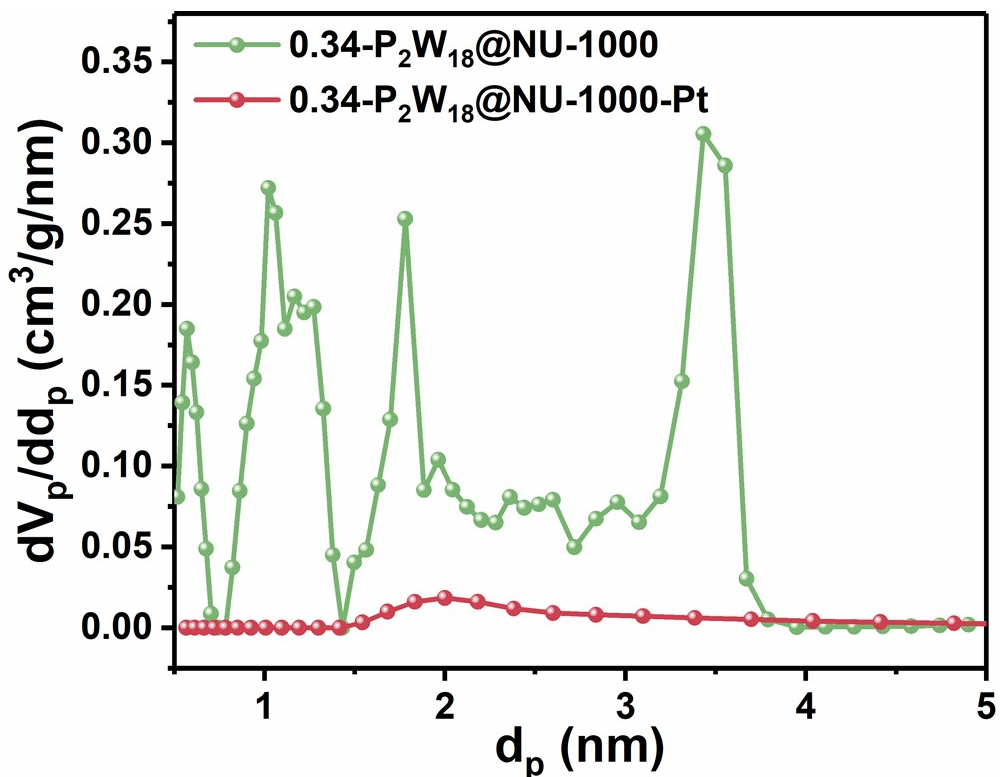


Figure S10. The comparison of the pore distribution curves of $0.34\text{-P}_2\text{W}_{18}\text{@NU-1000}$ before and after photocatalysis

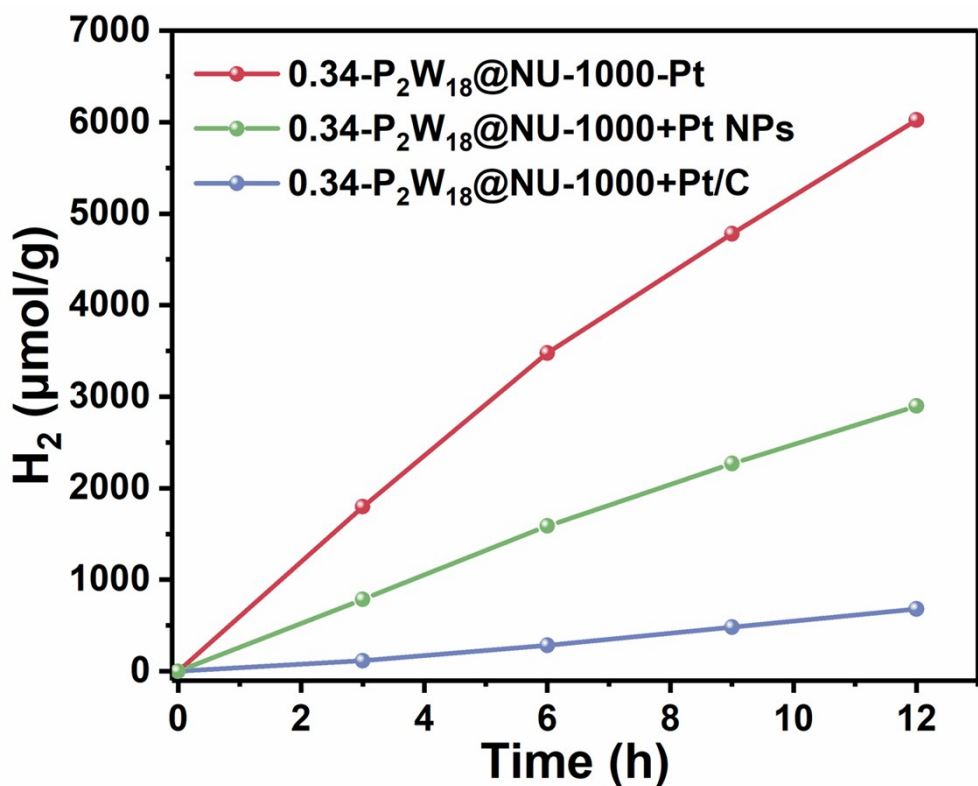


Figure S11. Photocatalytic hydrogen evolution of $0.34\text{-P}_2\text{W}_{18}\text{@NU-1000}$ with different types of Pt sources which contain equal amount of Pt species.

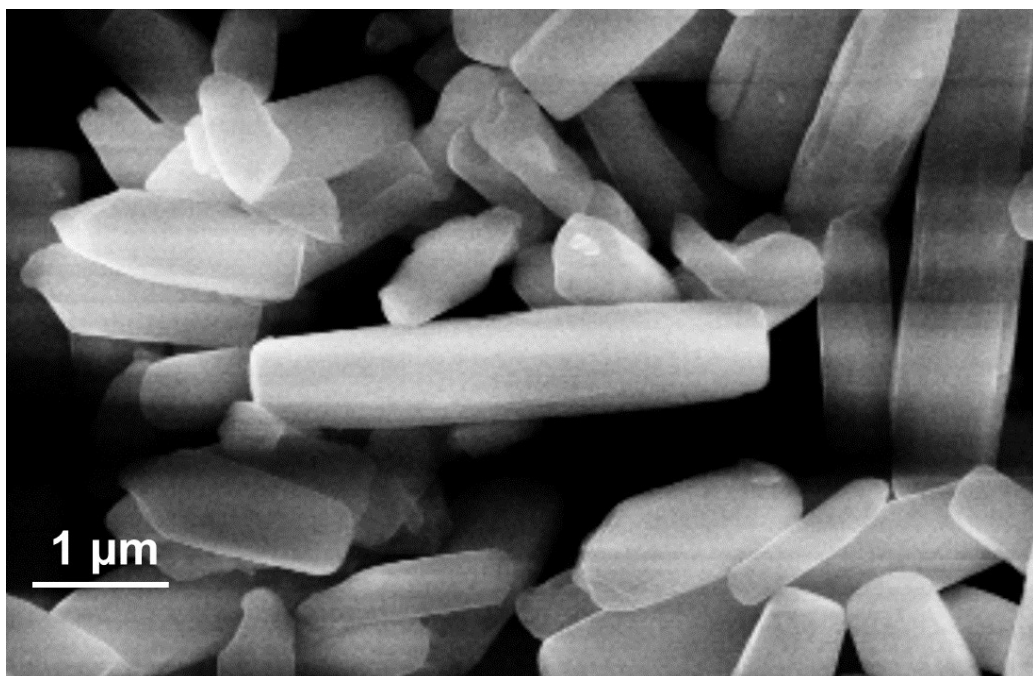


Figure S12. SEM image of $0.34\text{-P}_2\text{W}_{18}\text{@NU-1000}$ after photocatalytic hydrogen evolution for 12 h.

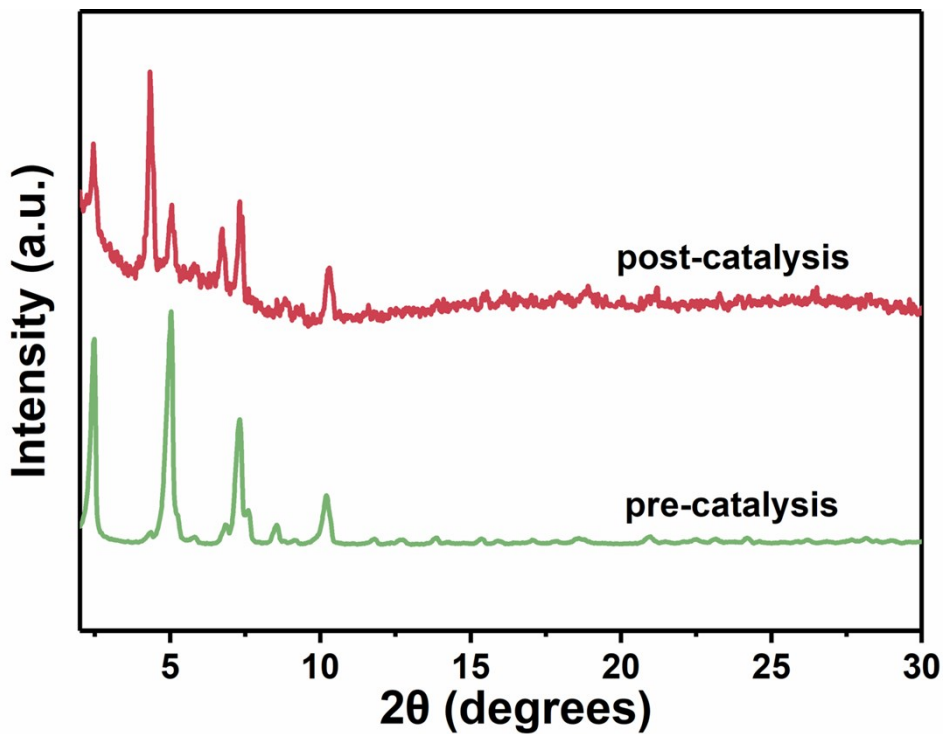


Figure S13. PXRD patterns of $0.34\text{-P}_2\text{W}_{18}\text{@NU-1000}$ before and after photocatalytic reaction for 12 h.

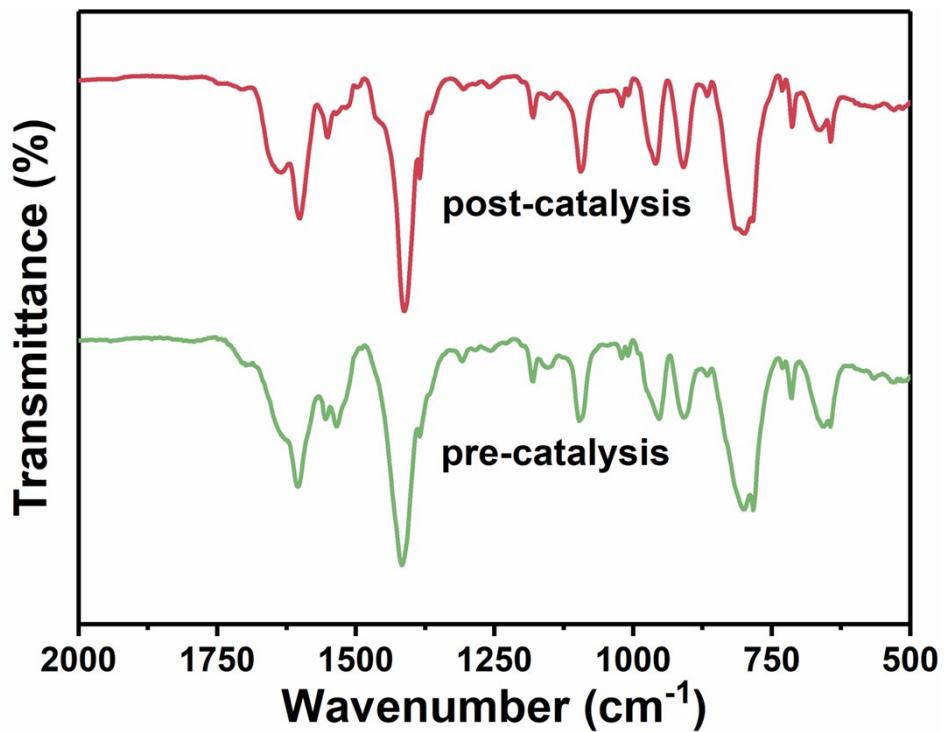


Figure S14. FT-IR spectra of $0.34\text{-P}_2\text{W}_{18}\text{@NU-1000}$ before and after photocatalysis for 12 h.

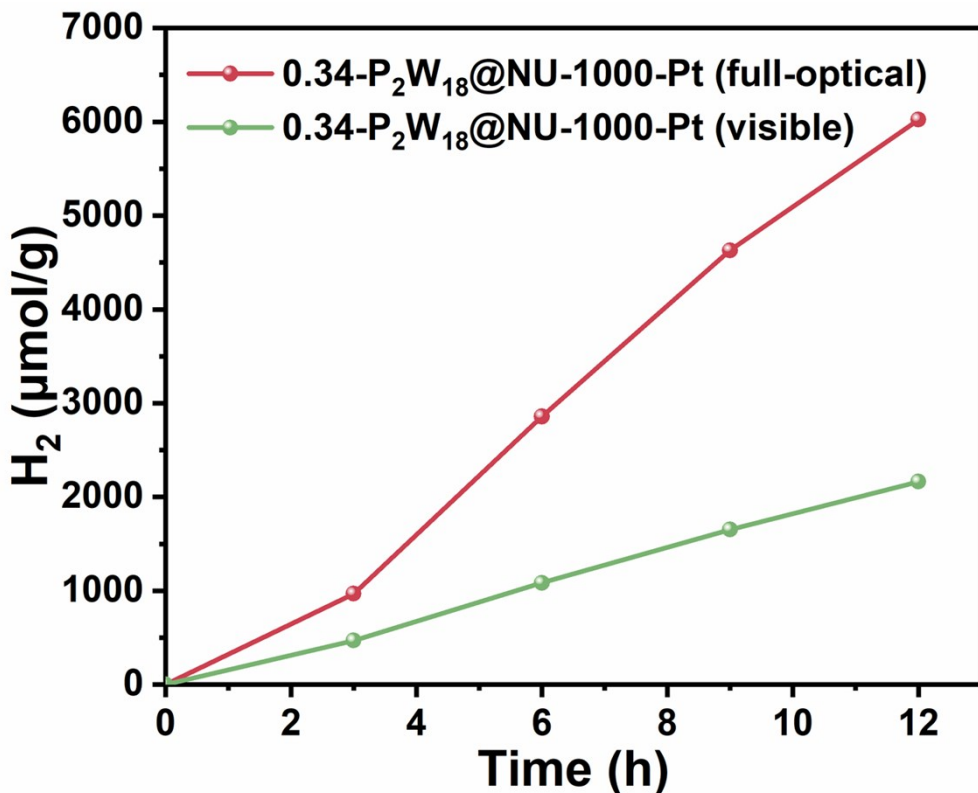


Figure S15. Photocatalytic hydrogen under different light sources. Reaction conditions: 10 mg of 0.34-P₂W₁₈@NU-1000, 0.25 wt% Pt, pH=5.5, 20 mL of 1 M AA aqueous, 300 W Xe-lamp.

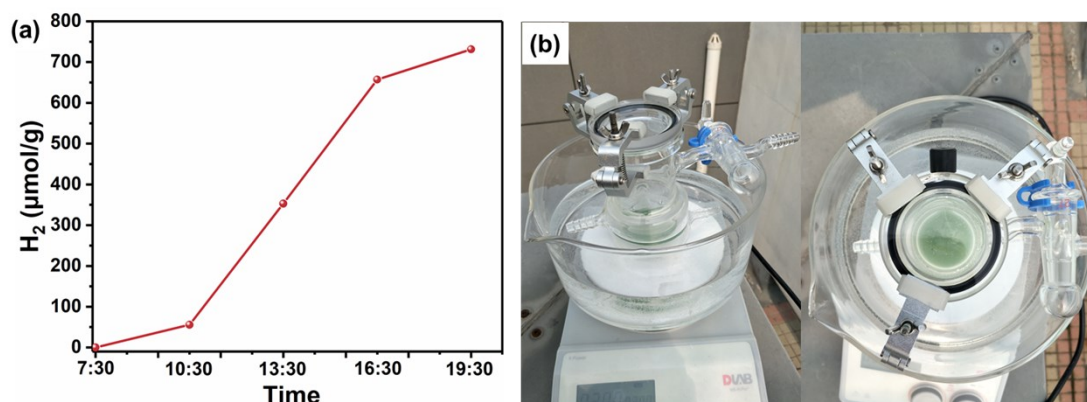


Figure S16. (a) Photocatalytic hydrogen evolution of 0.34-P₂W₁₈@NU-1000 under Natural Sunlight. Weather conditions (obtained from the website of China National Meteorological Observatory <http://www.weather.com.cn>): Beijing, China; N 39°43'29'', E 116°9'51''; ASL 130 m; July 15th, 2019; 34 °C/24 °C, Cloudy; Visibility: 4 km; UV intensity level (at noon): 7. Experiment conditions: 10 mg 0.34-P₂W₁₈@NU-1000 catalyst, 0.25 wt% Pt, 20 ml of 1 M AA aqueous at pH 5.5. (b) Photos of equipment for photocatalytic hydrogen evolution under Natural Sunlight.

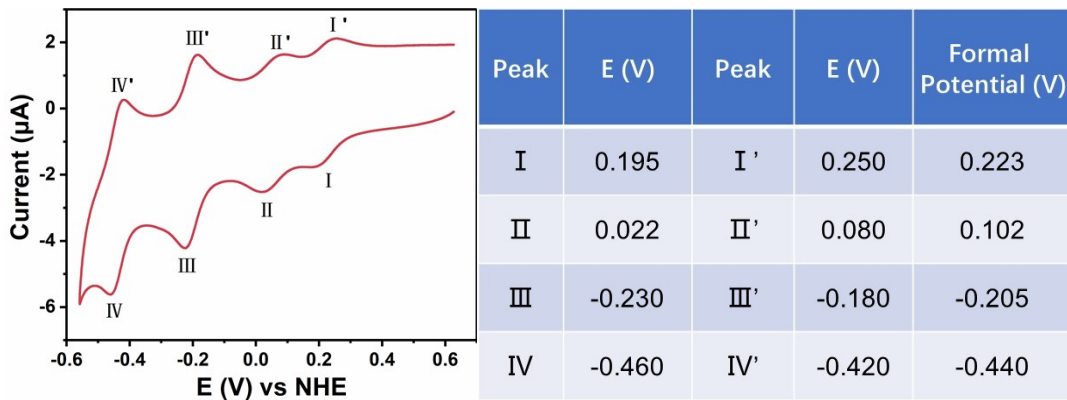


Figure S17. Left: Cyclic voltammogram of $\mathbf{P}_2\mathbf{W}_{18}$ (10^{-4} M) in 0.1 M H_2SO_4 aqueous solution using glassy carbon working electrode, saturated calomel electrode (SCE) reference electrode, and Pt wire auxiliary electrode; Right: the corresponding peak potentials and calculated formal potentials for different redox couples. Scan rate: 50 mV/s. The measured potential was expressed by converting to normal hydrogen electrode (NHE).

2. Table S1-S2

Table S1. Comparison of different photocatalytic systems for hydrogen production using POM@MOF composites. TON is defined as $n(1/2 \text{ H}_2)/n(\text{catalyst})$.

Catalyst	Photosensitizer	Solvent	Time	TON	Ref.
$\mathbf{P}_2\mathbf{W}_{18}@\text{NU-1000-Pt}$	—	H_2O	120 h	5464	This work
PNPMOF	—	H_2O	6 h	64	¹
$\mathbf{Ni}_4\mathbf{P}_2\mathbf{W}_{18}@\text{MOF-1}$	—	$\text{H}_2\text{O}/\text{MeOH}$	72 h	1476	²
$\mathbf{P}_2\mathbf{W}_{15}\mathbf{V}_3@\text{MIL-101}$	$[\text{Ru}(\text{bpy})_3]^{2+}$	$\text{DMF}/\text{H}_2\text{O}/\text{CH}_3\text{CN}$	8 h	56	³
WD-POM@SMOF-1	$[\text{Ru}(\text{bpy})_3]^{2+}$	$\text{H}_2\text{O}/\text{MeOH}$	12 h	392	⁴
$\mathbf{P}_2\mathbf{W}_{18}@\text{UiO}$	—	$\text{DMF}/\text{CH}_3\text{CN}$	14 h	307	⁵

Table S2. PL decay (at 505 nm) lifetimes of NU-1000, 0.34- $\mathbf{P}_2\mathbf{W}_{18}@\text{NU-1000}$ samples upon excitation at 365 nm, the PL decays were corrected by IRF.

Compounds	τ_1 (ns)	τ_2 (ns)	τ_3 (ns)
NU-1000	0.76	3.89	15.17
0.34-$\mathbf{P}_2\mathbf{W}_{18}@\text{NU-1000}$	0.53	3.01	13.23

3. Apparent quantum yield calculation

$$n_{\text{photons}} = \frac{Pt\lambda}{hcN_A} = 7.136 \times 10^{-3} \text{ mol} \quad (1)$$

$$\phi = \frac{2 \times n_{H_2}}{n_{\text{photons}}} = 1.69\% \quad (2)$$

Where P is the illumination power ($P=EA_R$, $E=2.6 \text{ mW/cm}^2$), A_R is the irradiation area (πR^2 , $R=2.1 \text{ cm}$), t is the illumination time (s, in our cases $t=43200 \text{ s}$), equivalent wavelength $\lambda=549 \text{ nm}$ for full optical Xe-lamp, h is the Planck constant, c is the velocity of light and N_A is Avogadro's number.

4. References

1. W. Guo, H. Lv, Z. Chen, K. P. Sullivan, S. M. Lauinger, Y. Chi, J. M. Sumliner, T. Lian and C. L. Hill, *J. Mater. Chem. A*, 2016, **4**, 5952-5957.
2. X. J. Kong, Z. Lin, Z. M. Zhang, T. Zhang and W. Lin, *Angew. Chem. Int. Ed.*, 2016, **55**, 6411-6416.
3. H. Li, S. Yao, H.-L. Wu, J.-Y. Qu, Z.-M. Zhang, T.-B. Lu, W. Lin and E.-B. Wang, *Appl. Catal. B: Environ.*, 2018, **224**, 46-52.
4. J. Tian, Z. Y. Xu, D. W. Zhang, H. Wang, S. H. Xie, D. W. Xu, Y. H. Ren, H. Wang, Y. Liu and Z. T. Li, *Nat. Commun.*, 2016, **7**, 11580.
5. Z. M. Zhang, T. Zhang, C. Wang, Z. Lin, L. S. Long and W. Lin, *J. Am. Chem. Soc.*, 2015, **137**, 3197-3200.